On the Relationship between Subduction Rates and Diabatic Forcing of the Mixed Layer

A. J. GEORGE NURSER AND JOHN C. MARSHALL

Space and Atmospheric Physics Group, Department of Physics, Imperial College, London, United Kingdom

(Manuscript received 14 September 1990, in final form 15 March 1991)

ABSTRACT

The transport of mass between a mixed layer, exposed to mechanical and thermodynamic forcing, and an adiabatic thermocline is studied for gyre-scale motions. It is shown that if the mixed layer can be represented by a vertically homogeneous layer, whose base velocity and potential density are continuous, then, at any instant, the rate at which fluid is subducted per unit area of the sloping mixed-layer base, S, is given by

$$S = \frac{\alpha_E f \mathscr{H}_{\text{net}}}{hC_w \bar{\rho} Q_b},$$

where h is the depth of the mixed layer, $Q_b = -f\bar{\rho}^{-1}\partial\rho/\partial z|_{z=-h}$ is the large-scale potential vorticity at its base, $\mathscr{H}_{\text{net}}$ is the heat input per unit area less that which warms the Ekman drift, and α_E, C_w, and $\bar{\rho}$ are the volume expansion coefficient, heat capacity, and mean density of water, respectively. It is assumed that the mixed layer is convectively controlled and much deeper than the layer directly stirred by the wind. The field of S is studied in a steady thermocline model in which patterns of Ekman pumping and diabatic heating drive flow to and from a mixed layer overlying a stratified thermocline.

1. Introduction

Our ways of thinking about the subtropical gyre are dominated by the idea that surface waters are pumped down into—"ventilate"—the main thermocline under the action of the prevailing winds: in classical thermocline theory the Ekman pumping field w_e is prescribed at the base of the Ekman layer (Fig. 1), and this is the velocity with which fluid passes into the main thermocline. In reality, of course, the Ekman layer merely pumps fluid down into a mixed layer, and it is the mass flux, S, through the sloping and time-varying base of the mixed layer that ventilates the main thermocline (Fig. 1). In this contribution we are concerned with understanding which factors determine the sense and magnitude of S, and how it is related to w_e, and the dynamics and thermodynamics of the mixed layer. In particular, we study how, on the large scale, a vertically isothermal mixed layer, exposed to wind and thermal forcing, interacts with an "ideal" thermocline, shielded from any forcing.

Under the action of mechanical and diabatic forcing the mixed layer may cool and burrow into the thermocline, "entraining" thermocline waters; stratification existing in the thermocline determines how the mixed layer responds to the applied forcing. Alternatively, the mixed layer may warm and retreat, leaving behind newly stratified fluid, thus setting the stratification of the thermocline. As the mixed layer deepens and shallows, the gyre sweeps fluid to and from the main thermocline through the base of the sloping mixed layer. So the flux of mass between the mixed layer and the thermocline depends on both the "up–down" motion of the mixed layer and the "sideways" motion of the gyre sliding fluid across the sloping base of the mixed layer.

In section 2, we derive and discuss the relationship quoted in the Abstract, relating the subduction flux S to the large-scale parameters. In section 3 we use the steady thermocline model described in Marshall and Nurser (1991, hereafter MN) to illustrate our ideas in an idealized context. In section 4 we discuss the implications of our work to illustrate of the interaction between a deepening and shallowing mixed layer and a stratified thermocline.

2. Subduction and entrainment

a. *The mass flux between the mixed layer and the thermocline*

We adopt the mixed layer and stratified thermocline represented schematically in Fig. 1, which is in accord with the idealization presented in Woods (1985). We assume that the layer directly driven by the wind (the Ekman layer) is shallow relative to the depth of the mixed layer. Furthermore, we assume that density and velocity are continuous at the base of the mixed layer.

Corresponding author address: Dr. J. C. Marshall, Dept. of Earth, Atmospheric and Planetary Sciences, Massachusetts Institute of Technology, Cambridge, MA 02139.

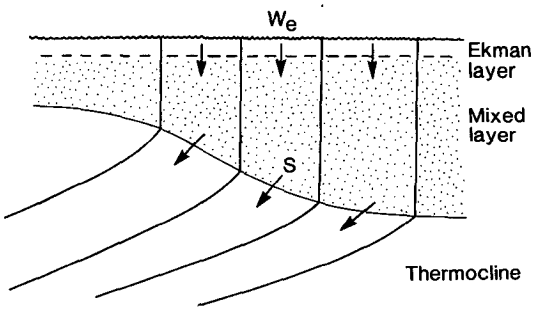

FIG. 1. A schematic diagram showing isopycnals in the thermocline outcropping into a vertically homogeneous mixed layer. Ekman pumping at the surface w_e drives horizontal flow in the mixed layer, which slides to and from the thermocline through the sloping base of the mixed layer. The mass flux per unit surface area through the mixed-layer base is S; it is the field of S that drives flow in the thermocline.

This assumption is perhaps most appropriate to a deep winter mixed layer. The flow in the thermocline is supposed to be adiabatic. Our analysis permits time dependence.

Following Cushman-Roisin (1987) and Williams (1989), consider a fluid parcel that at time $t = t_o$ lies (Fig. 2) at the base of the mixed layer, with horizontal position $\mathbf{x}_o = (x_o, y_o)$ and vertical position $z = -h(x_o, y_o, t_o)$, where $h(x, y, t)$ is the thickness of the mixed layer, and x, y, and z are the eastward, northward, and upward coordinates of a local Cartesian frame. Let the fluid parcel have horizontal velocity $\mathbf{u}_b = (u_b, v_b)$ and vertical velocity w_b. Then, after a time Δt, it moves a distance Δz_d below the mixed-layer base, where

$$\Delta z_d = -\frac{\partial h}{\partial t}\Delta t - (\mathbf{u}_b\Delta t)\cdot\nabla h - w_b\Delta t$$

and

- $-\partial h/\partial t\cdot\Delta t$ is the distance that the mixed-layer base has moved upward in time Δt;
- $-(\mathbf{u}_b\Delta t)\cdot\nabla h$ takes account of the fact that the mixed layer is shallower above the new horizontal position $\mathbf{x}_o + \mathbf{u}_b\Delta t$ of the fluid parcel; and
- $-w_b\Delta t$ is the distance traveled downward as a result of the vertical velocity of the fluid parcel.

Thus defining S, the subduction velocity to be the downward velocity of the parcel (following the horizontal motion of the parcel) relative to the base of the mixed layer:

$$S = \frac{\Delta z}{\Delta t} = -\frac{\partial h}{\partial t} - \mathbf{u}_b\cdot\nabla h - w_b.$$

In terms of

$$\frac{D_b}{Dt} = \frac{\partial}{\partial t} + \mathbf{u}_b\cdot\nabla,$$

the Lagrangian derivative following the horizontal component of the flow at the base of the mixed layer, S can be written:

$$S = -w_b - \frac{D_b h}{Dt}. \tag{1}$$

Thus S is equal to the downward velocity of the fluid parcel less the rate, following the horizontal motion of that parcel, at which the mixed layer deepens.

The subduction velocity S gives the rate per unit horizontal area at which water is subducted into the thermocline from the mixed layer. For example, consider a prism lying across the mixed-layer base with a cross-sectional area (perpendicular to the z axis; i.e., parallel to the ocean surface) dA (see Fig. 3). Then the area of mixed-layer base enclosed within this prism dA' has upward *unit* normal $\mathbf{n}$, where

$$\mathbf{n} = \frac{\mathbf{k} + \nabla h}{\sqrt{1 + (\nabla h)^2}}$$

$$dA' = dA\sqrt{1 + (\nabla h)^2}.$$

The three-dimensional velocity of the fluid relative to the mixed-layer base, which is moving upward with vertical velocity $-\partial h/\partial t$, is $\mathbf{u}_3 \equiv (\mathbf{u}_b, w_b + \partial h/\partial t)$. Therefore, S', the flux of water into the thermocline per unit area of the mixed-layer base, is given by $S' = -\mathbf{u}_3\cdot\mathbf{n}$. Then the total flux across the mixed-layer base area, dA' in Fig. 3, is

$$S'dA' = -\mathbf{u}_3\cdot\mathbf{n}dA' = -\mathbf{u}_3\cdot(\mathbf{k} + \nabla h)dA = SdA,$$

using the definition of S in (1).

Thus, S gives the rate at which water is subducted per unit horizontal area. In fact, the mixed-layer slope $|\nabla h|$ is generally $O(10^{-4})$ and even in frontal regions is unlikely to exceed $1/100$. Thus, $dA \approx dA'$ and so $S \approx S'$: for all practical purposes S may be considered as the rate of subduction per unit area of the mixed-layer base.

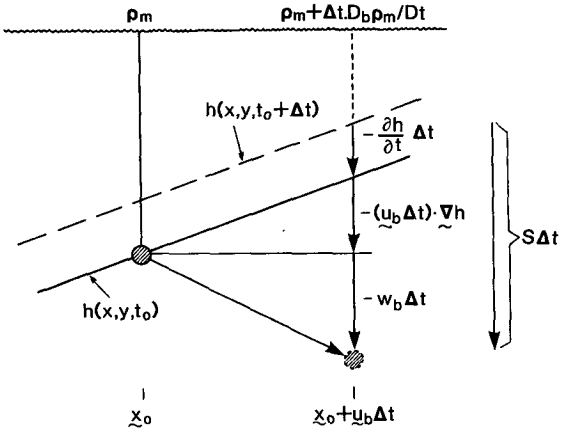

FIG. 2. A schematic diagram showing a particle being subducted from the time-varying base of the mixed layer into the thermocline below.

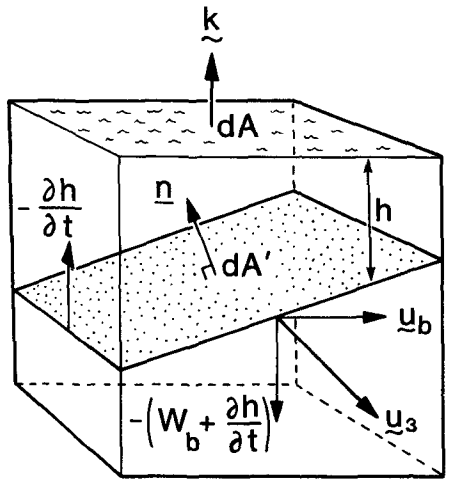

FIG. 3. A schematic diagram relating S to the mass flux/unit area through the base of the sloping mixed layer.

As we shall now show, S can be related to the stratification, $\partial\rho/\partial z$, of the water, which is entrained by the mixed layer or subducted into the thermocline, and $D_b\rho_m/Dt$, the Lagrangian rate of change of the mixed-layer density ρ_m.

Consider again the subducted fluid parcel in Fig. 2, which now lies a distance $-S\Delta t$ below the base of the mixed layer. Because it has traveled through the adiabatic thermocline, it retains its initial density ρ_m. However, the density of the mixed layer immediately above the new position of the parcel has a value $\rho_m + \Delta t D_b\rho_m/Dt$. Hence, the density gradient of the newly subducted water is

$$\left.\frac{\partial\rho}{\partial z}\right|_{z=-h} = \frac{D_b\rho_m}{Dt}\Big/ S \tag{2}$$

or, rearranging,

$$S = \frac{D_b\rho_m}{Dt}\Big/\left.\frac{\partial\rho}{\partial z}\right|_{z=-h}.$$

If the thermocline is to be stably stratified, $\partial\rho/\partial z$ *must be negative.* Therefore, (2) implies that subduction ($S > 0$) is only possible if $D_b\rho_m/Dt < 0$; fluid at the base of the mixed layer is becoming less dense. A fluid parcel previously in the mixed layer can only find itself beneath the mixed layer if fluid parcels at the base of the mixed layer, which are traveling with the same velocity as the parcel of subducted fluid, become less dense.

Conversely, for entrainment to occur, water that was previously denser than the mixed layer must find mixed-layer water of the same density above it. The mixed-layer base must become denser, following the motion, with $D_b\rho_m/Dt > 0$ if there is to be entrainment, with $S > 0$.

A simple mixed layer is now described that allows (2) to be reformulated in terms of the applied heating and the potential vorticity field in the thermocline.

b. Subduction and entrainment in a simple mixed layer

The mixed layer is vertically homogeneous, with density $\rho_m(x, y, t)$ and thickness $h(x, y, t)$. It is exposed to thermal and mechanical forcing. Mechanical forcing is confined to a thin surface Ekman layer; below this Ekman layer the flow is assumed to be in geostrophic and hydrostatic balance:

$$\mathbf{u}_m = \mathbf{k} \times \nabla p_m/(\bar{\rho} f) \tag{3}$$

$$\frac{\partial p_m}{\partial z} + g\rho_m = 0. \tag{4}$$

Thus, time scales have been assumed to be much longer than the inertial time scale f^{-1}.

1) THE THERMODYNAMIC EQUATION

No jump in density is permitted between the base of the mixed layer and the thermocline. Therefore there is no "entrainment flux": the density balance of the layer is

$$-\frac{1}{\bar{\rho} f}\,\mathbf{k} \times \tau \cdot \nabla\rho_m + \int_{-h}^{0} \frac{D_g\rho_m}{Dt}\,dz = -\frac{\mathcal{B}}{g}. \tag{5}$$

Here τ is the applied wind stress, and

$$\mathcal{B} = g\left(\frac{\alpha_E \mathscr{H}_{\text{in}}}{C_w} + \beta_S \mathcal{S}\mathcal{F}\right)$$

is the buoyancy forcing, which includes the heat input/unit surface area $\mathscr{H}_{\text{in}}$, and the freshwater influx/unit area $\mathcal{F}$; α_E is the thermal expansion coefficient, β_S the corresponding coefficient for salinity $\mathcal{S}$, and C_w the specific heat of water.

The material rate of change, $D_g\rho_m/Dt$, follows the *geostrophic* flow $\mathbf{u}_m$. We have thus assumed that advection of density by the components of the ageostrophic flow, other than the Ekman flux, is unimportant.

To keep the exposition simple, buoyancy inputs resulting from freshwater fluxes are now neglected, so $\mathcal{B}$ reduces to $g\alpha_E\mathscr{H}_{\text{in}}/C_w$. Buoyancy input is thus synonymous with heat input.

A key quantity is the net heating $\mathscr{H}_{\text{net}}$, the surface heat input less that component that warms the Ekman drift:

$$\mathscr{H}_{\text{net}} = \mathscr{H}_{\text{in}} - \frac{C_w}{\alpha_E\bar{\rho} f}\,\mathbf{k} \times \tau \cdot \nabla\rho_m. \tag{6}$$

Expressed in terms of $\mathscr{H}_{\text{net}}$, (5) simplifies to

$$\int_{-h}^{0} \frac{D_g\rho_m}{Dt}\,dz = -\frac{\alpha_E\mathscr{H}_{\text{net}}}{C_w}. \tag{7}$$

By geostrophy and hydrostasy, the velocity shear is in thermal wind balance, so

$$\mathbf{u}_m = \mathbf{k} \times \nabla p_s/(\bar{\rho} f) - gz\mathbf{k} \times \nabla \rho_m/(\bar{\rho} f), \quad (8)$$

where the surface pressure is $p_s = p|_{z=0}$. Thus, the component of mixed-layer velocity along the temperature gradient is uniform throughout the mixed layer. *The advection* $\mathbf{u}_m \cdot \nabla \rho_m$, *and hence* $D_g\rho_m/Dt$, *is independent of depth throughout the mixed layer.*

By dividing (7) through by h,

$$\frac{D_g\rho_m}{Dt} = -\frac{\alpha_E \mathscr{H}_{\text{net}}}{hC_w}. \quad (9)$$

The material rate of change of density, $D_g\rho_m/Dt$ anywhere in the mixed layer is equal to the density flux convergence $\alpha_E\mathscr{H}_{\text{net}}/(hC_w)$. The steady form of the thermodynamic equation (9) is the key equation of the model described in MN.

2) Relating S to the diabatic heating

Equation (9) enables S to be expressed in terms of the net heating. In particular, it holds at the mixed-layer base $z = -h$. Because the Ekman flux is confined to a thin surface layer, this geostrophic material derivative is equal to the *total* material derivative at the base of the mixed layer:

$$\left.\frac{D_g\rho_m}{Dt}\right|_{z=-h} = \frac{D_b\rho_m}{Dt}.$$

Hence, $D_b\rho_m/Dt$ is related directly to the net heating:

$$\frac{D_b\rho_m}{Dt} = -\frac{\alpha_E \mathscr{H}_{\text{net}}}{hC_w}. \quad (10)$$

Therefore, $D_b\rho_m/Dt$ may be eliminated from (2), and the subduction velocity expressed in terms of the net heating and the stratification at the base of the mixed layer:

$$S = -\frac{\alpha_E \mathscr{H}_{\text{net}}}{hC_w \partial\rho/\partial z|_{z=-h}}. \quad (11)$$

In terms of the large-scale potential vorticity, $Q_b = -f\bar{\rho}^{-1}\partial\rho/\partial z|_{z=-h}$ (11) may be expressed:

$$S = \frac{\alpha_E f \mathscr{H}_{\text{net}}}{\bar{\rho} hC_w Q_b}. \quad (12)$$

Equation (12) is the main result of the present study; it is a remarkable relationship, showing that subduction/entrainment is proportional to the strength of the net cooling/heating modulated by the thickness of the mixed layer and the stratification at the base of the mixed layer. Furthermore, it asserts that the flux of potential vorticity between the mixed layer and the thermocline, SQ_b, is simply proportional to $f\mathscr{H}_{\text{net}}/h$.

It is worth noting, that it is the net heating, $\mathscr{H}_{\text{net}}$, that appears in Eq. (12) and controls S, rather than $\mathscr{H}_{\text{in}}$, the total heating; $\mathscr{H}_{\text{net}}$ will be zero if $\mathscr{H}_{\text{in}}$ supplies just sufficient heat to allow the Ekman drift to cross the surface density contours. In this case, $S = 0$ and there can be no transfer of mass between the mixed layer and the thermocline. However, if there is net cooling $S < 0$ (entrainment); if there is net heating $S > 0$ (subduction).

In the thermocline solutions presented in MN, only when $\mathscr{H}_{\text{net}} \neq 0$ is there a transfer of mass. In those steady solutions in which $\mathscr{H}_{\text{net}} = 0$, then the geostrophic flow in the mixed layer is always parallel to the ρ_m contours and $S = 0$.

In view of the fact that the wind stress does not explicitly appear in Eq. (12), it is ironic that the seminal paper on the ventilated thermocline (Luyten et al. 1983, hereafter LPS) appears at first sight to be purely wind driven. Furthermore, it has a mixed layer of zero depth. In fact, diabatic processes are implicit in the formulation: in the special case of LPS, both $\mathscr{H}_{\text{net}}$ and $h \to 0$ but the heat flux *convergence* $\mathscr{H}_{\text{net}}/h$ remains finite with $S = -w_e$, the Ekman pumping.

It should be mentioned that Frederiuk and Price (1985) and Woods and Barkmann (1988) were aware of the intimate connection between subduction and diabatic processes; in their seasonally forced Lagrangian mixed-layer model, fluid passes permanently from the mixed layer into the thermocline as the parcel moves from regions of net cooling to regions of net warming. Equation (12) makes the connection with the diabatic forcing explicit and quantitative.

In the next section a steady thermocline model is employed, described in the accompanying paper, MN, to explore further the dependence of S on the heating field, the mixed-layer depth, and the stratification at the base of the mixed layer.

3. Subduction and entrainment in a steady thermocline model

In the companion paper to this contribution, MN, we have set out and presented solutions from a model that couples the steady geostrophic mixed layer of section 2b with an ideal thermocline. In that model, the potential vorticity of fluid in motion within the thermocline is specified; in particular, it is assumed to be uniform on each isopycnal surface. This assumption allows a complete solution to be found, given only the wind stress and applied surface heating; the formulation is ideally suited to study the "sliding" motion of fluid across the mixed-layer base.

In MN, steady solutions for the thermocline and mixed layer were presented in response to fields of Ekman pumping. Here a pattern of cooling and warming is superimposed, which allows transfer of fluid between the mixed layer and the thermocline. We shall illustrate the dependence of this transfer rate, S, on the mixed-layer depth and the stratification at the base of the mixed layer. First, in section 3a, we consider solutions

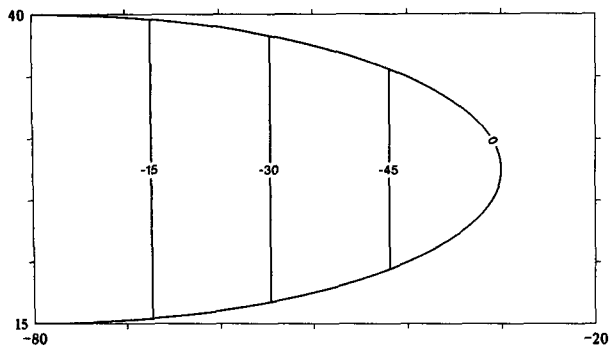

FIG. 4. The Ekman forcing applied to the subtropical gyre in meters per year. The model subtropical gyre extends from 15° to 40°N and from 80° to 20°W.

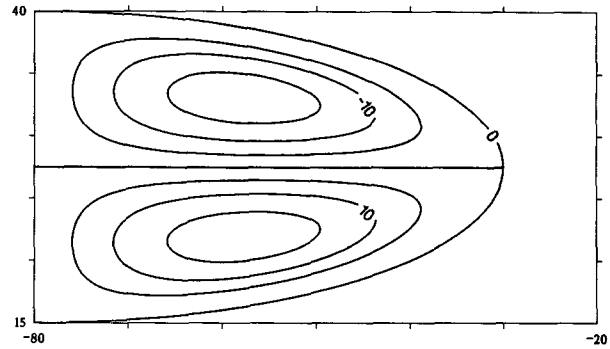

FIG. 6. Contours of the net heat input to the mixed layer, in W m^{-2}. There is cooling to the north and warming to the south.

in which the mixed layer has a finite thickness and then go on, in section 3b, to study the degenerate case when there is no mixed layer, as in LPS or Rhines and Young (1982).

Note that the model is formulated in full spherical geometry, with latitude θ and longitude λ.

a. A mixed layer of finite thickness

To illustrate our ideas in a simple framework we choose a very idealized distribution of wind forcing: an Ekman pumping restricted to the eastern half of a disk, whose strength is proportional to the distance east of the disk's center. This drives a depth-integrated flow of circular form if, as supposed by Rhines and Young (1982), the disk is circular. We, however, differ in choosing a disk that is elliptical, with greater zonal than meridional extent. This allows realistic Ekman pumping velocities (typically 30 m yr^{-1}) to drive a reasonably strong ($\sim$15 Sv; Sv $\equiv 10^6$ m^3 s^{-1}) gyre. Thus (see Fig. 4), inside the half-disk, "center" $\lambda_c = -80°$, $\theta_c = 27.5°$, semimajor axis $a = 50°$, and semiminor axis $b = 12.5°$:

$$w_e = w_e^*(\lambda - \lambda_c)/a \qquad (13a)$$

while outside of this disk, where there is no flow,

$$w_e = 0. \qquad (13b)$$

We choose a maximum Ekman pumping velocity at the extreme eastern margin of the gyre of $w_e^* = 60$ m yr^{-1}. This Ekman pumping field (13) drives, through the Sverdrup constraint, a barotropic flow of broadly elliptical form (see Fig. 5).

In addition, we apply a net heating field

$$\mathscr{H}_{\text{net}} = \mathscr{H}^*_{\text{net}} \frac{\lambda - \lambda_c}{a} \frac{\theta - \theta_c}{b} F_{\text{gauss}}(r) \qquad (14)$$

while $\mathscr{H}^*_{\text{net}} = 200$ W m^{-2} is a prescribed constant, and

$$r = \left[\left(\frac{\lambda - \lambda_c}{a}\right)^2 + \left(\frac{\theta - \theta_c}{b}\right)^2\right]^{1/2}.$$

Here $F_{\text{gauss}}(r)$ is chosen to have the form of a Gaussian, vanishing at $r = 1$:

$$F_{\text{gauss}}(r) = \frac{1}{1 - c}(e^{-r^2} - c),$$

if $r < 0.9$ and

$$F_{\text{gauss}}(r) = d(1 - r)^2,$$

if $r > 0.9$.

The constants c and d are chosen to ensure continuity of F_{gauss} and its derivative at $r = 0.9$. The above heating field is plotted in Fig. 6. For positive $\mathscr{H}^*_{\text{net}}$, the northern ($\theta > \theta_c = 27.5°$) half of the gyre is cooled and the southern ($\theta > \theta_c = 27.5°$) half warmed; the maximum amplitude of the forcing is $\sim$18 W m^{-2}, perhaps a little weak, but not inconsistent with annual mean observations over the subtropical gyre of the North Atlantic (Isemer and Hasse 1987). Results from three different runs are shown.

In the first, a weak stratification is chosen at the base of the mixed layer, opening the "throat"[1] of the ther-

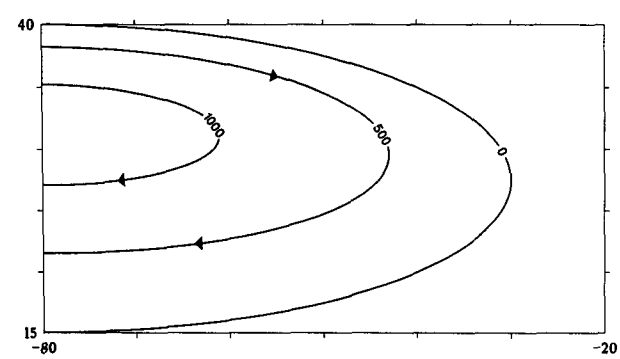

FIG. 5. Contours of depth-integrated perturbation pressure P', the streamfunction for the Sverdrup transport (see MN, section 2c), units: 10^3 N m^{-1}.

[1] We are using Rhines' (1986) terminology, in which the "mouth" represents the area at the sea surface between outcropping isopycnals and the "throat" the thickness between those isopycnals in the thermocline.

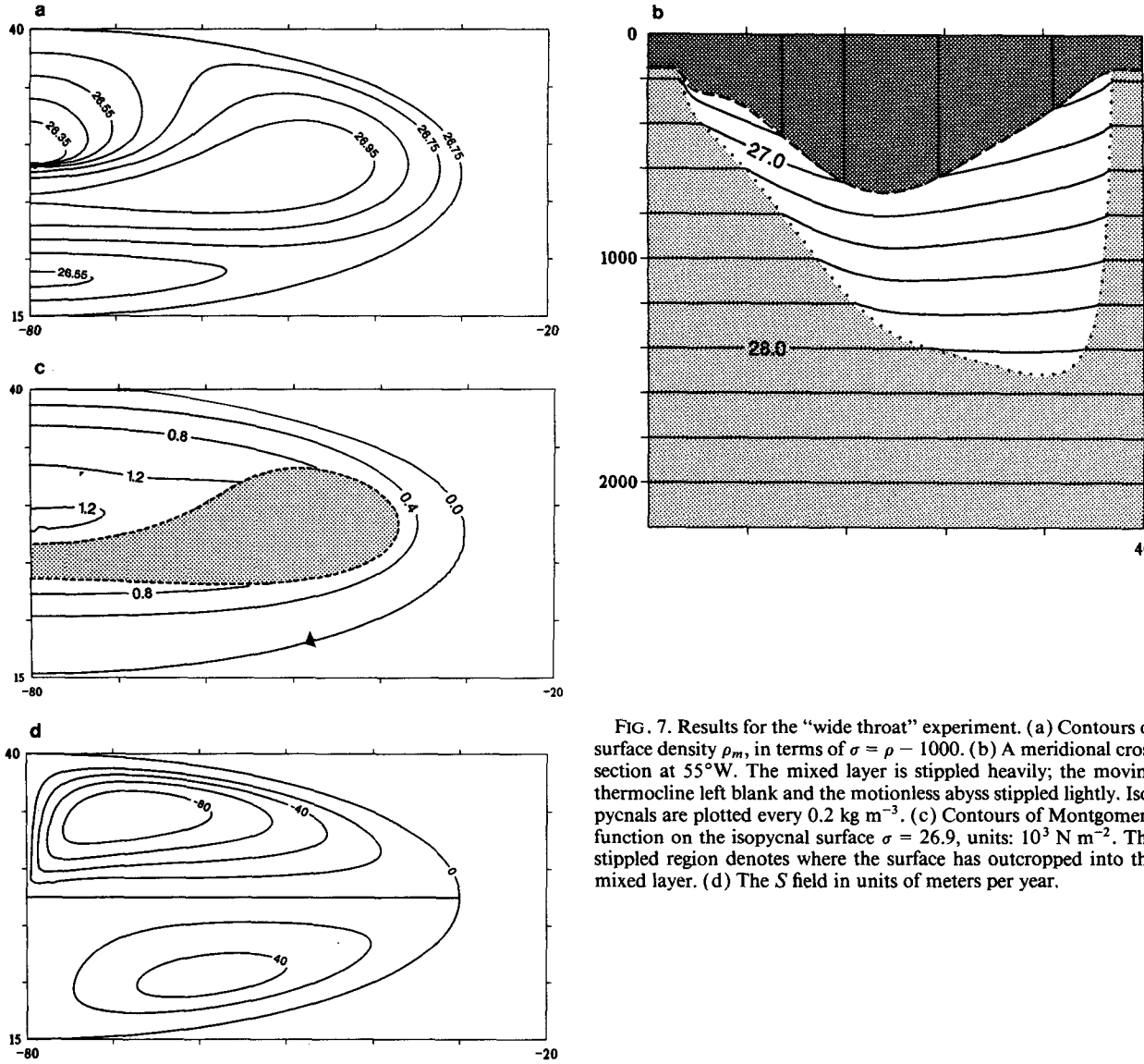

FIG. 7. Results for the "wide throat" experiment. (a) Contours of surface density ρ_m, in terms of $\sigma = \rho - 1000$. (b) A meridional cross section at 55°W. The mixed layer is stippled heavily; the moving thermocline left blank and the motionless abyss stippled lightly. Isopycnals are plotted every 0.2 kg m^{-3}. (c) Contours of Montgomery function on the isopycnal surface $\sigma = 26.9$, units: 10^3 N m^{-2}. The stippled region denotes where the surface has outcropped into the mixed layer. (d) The S field in units of meters per year.

mocline wide; in the second, we close the throat by increasing the stratification. These first two experiments are designed to illustrate the principles involved; they are not realistic simulations, particularly with respect to the deep mixed layers chosen. In the third experiment a slightly more realistic simulation is attempted, albeit in our rather idealized framework.

1) WIDE THROAT

We choose as our "reference" stratification—i.e., that which obtains outside the bowl of moving fluid and which, at the latitude of zero Ekman pumping, $f = f_o$, sets the value of potential vorticity on each surface—the uniform stratification given in Eq. (27) of MN:

$$\rho = \rho_{\text{ref}} - B(z - z_{\text{ref}}),$$

where $\rho_{\text{ref}} = 1027.0$ at $z_{\text{ref}} = -400$ m, and the uniform density gradient, $B = 1$ kg m^{-3}/km. This uniform density gradient implies that not only is potential vorticity in the moving thermocline uniform on isopycnals but that this uniform value is equal on all isopycnals. We choose a reference value of the mixed-layer density; i.e., that outside the gyre $\rho_{mo} = 1026.75$, as in MN.

To help prevent the mixed layer from becoming too deep, we choose the inflow condition on the northwestern boundary [MN, (28)]:

$$\rho_m = \rho_{mo} - 0.05 \times (40 - \theta°), \qquad (15)$$

where $\theta°$ is the latitude, measured in degrees. This in-

troduces a warm, thin, mixed layer into the center of the gyre.

The surface density field, Fig.7, that develops as the inflow from the northwestern boundary is cooled and then warmed by the surface heating field of Fig. 6. The warm, light patch toward the south of the inflow region is soon cooled and made dense. The meridional section, Fig. 7b, taken across the gyre at 55°W, shows the bulging down of the mixed layer where it has become dense, across the middle of the gyre. The outcropping of the isopycnal surfaces into the mixed layer is very striking.

The flow on the $\sigma = 26.9$ surface ($\sigma = \rho - 1000$) (Fig. 7c) is swallowed up by the cooling, deepening mixed layer and is then resubducted on the southern flank of the gyre as the mixed layer warms and shallows. To help visualize the flow, Fig. 8 presents a perspective plot of the flow on the $\sigma = 26.9$ surface. The field of S, the subduction velocity, is plotted in Fig. 7d; values range from 48 m yr^{-1} of subduction in the south to almost 100 m yr^{-1} of entrainment on the northern side of the gyre. The lower rates of subduction compared with entrainment arise from the uniformity of potential vorticity within the moving thermocline, which implies that the stratification is stronger where f is smaller; i.e., on the southern flank of the gyre. As the mixed-layer thickness is fairly symmetrical about the center of the gyre, then by Eq. (11), this stronger stratification weakens the subduction.

In terms of the argument illustrated in Fig. 2, $D_b\rho_m/Dt \cdot \Delta t = -\alpha_E \mathscr{H}_{\text{net}}/hC_w\Delta t$ specifies the difference in density after a time Δt between the mixed layer and the subducted fluid. However, where the required stratification, $-\partial\rho/\partial z$ of the thermocline is greater, the distance $-S\Delta t$, by which the parcel is pushed under the mixed layer, must be smaller; fluid is subducted into the thermocline at a slower rate.

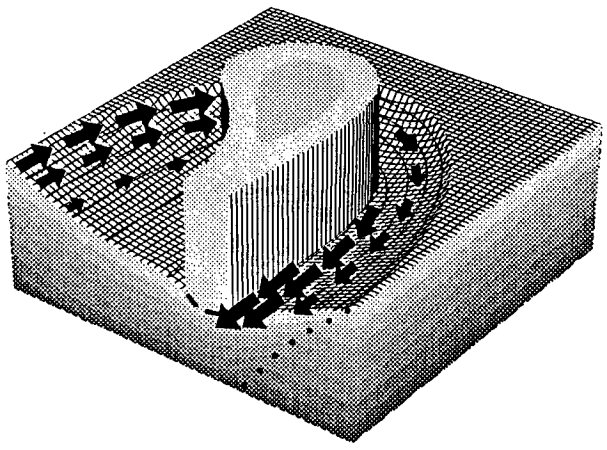

FIG. 8. A perspective plot of the upper 1000 m of the subtropical gyre, viewed from the southwest. The $\sigma = 26.9$ surface appears as a net; its depth is contoured every 25 m. The velocities on this surface are proportional to the length of the arrows. The "wall" denotes where the $\sigma = 26.9$ surface outcrops into the mixed layer.

A grey scale is used to represent the density field, both on the surface of the mixed layer and on the vertical planes. Each element of the grey scale covers a density range of 0.1 kg m^{-3}. The mixed-layer base is delineated by a dashed line, and the "bowl" by the dotted line.

Note the spectacular contrast between the S field (Fig. 7d) and the Ekman pumping field (Fig. 4), which is induced by the simple, steady mixed layer in this model. The S field broadly reflects the net heating field $\mathscr{H}_{\text{net}}$ but is now modulated by the stratification at the base of the mixed layer; it is only indirectly related to the Ekman pumping.

2) NARROW THROAT

We now assume a reference stratification that steepens toward the surface (Nurser 1988):

$$\rho = \rho_{\text{ref}} + \frac{\bar{\rho} s^2}{g}\left(\frac{1}{H_{\text{virt}} - z_{\text{ref}}} - \frac{1}{H_{\text{virt}} - z}\right), \quad (16)$$

where we choose $\rho_{\text{ref}} = 1027.0$ at $z_{\text{ref}} = -400$ m, and $s = 2.8$ m s^{-1} and $H_{\text{virt}} = 150$ m. This stratification now leads to a potential vorticity field, which while still uniform on each isopycnal, takes different values on different isopycnals.

As in the previous section, $\rho_{mo} = 1026.75$. However, we now suppose that the fluid enters the gyre from the northwest with uniform density $\rho_m = \rho_{mo} = 1026.75$. The surface density field that now develops is pictured in Fig. 9a and is similar to the corresponding field Fig. 7a of the previous section, but now there is no warm patch on the western boundary. The meridional section across the gyre at 55°W (Fig. 9b) shows, again, the mixed-layer bulging down in the center of the gyre. Note the steepening of the stratification on the lighter isopycnals; in the center of the cross section, where $\rho_m \approx 1027.0$, $\partial\rho/\partial z \approx 2.4$ kg m^{-3}/km, while at the edges where $\rho_m \approx 1026.8$, $\partial\rho/\partial z \approx 3.5$ kg m^{-3}/km. The stratification at the base of the mixed layer is everywhere considerably steeper than in the case with uniform stratification, where it was 1 kg m^{-3}/km.

Since the thickness of the mixed layer is roughly the same, the net heating (which is identical to that used in section 3a) is much less effective in driving subduction and entrainment. Values range (Fig. 9c) from 12 m yr^{-1} of subduction on the southern flank to 18 m yr^{-1} of entrainment over the northern. The stronger stratification lessens the quantity of fluid subducted for the same heat input.

3) A THINNER MIXED LAYER

The above two cases have been chosen to illustrate the dependence of the subduction rate upon the stratification rather than for realism. We now choose parameters so as to produce a thinner, more realistic, mixed layer. We again choose the surface-intensified reference stratification, but because the mixed layer is

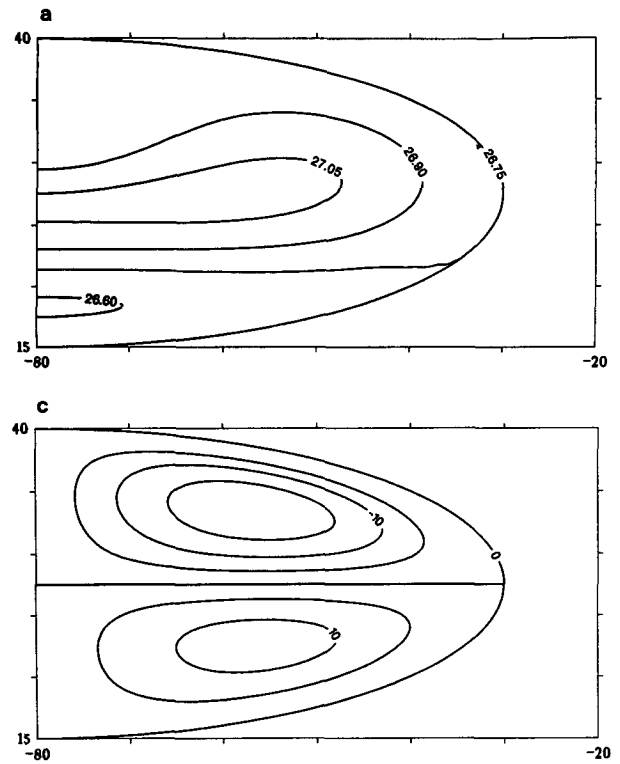

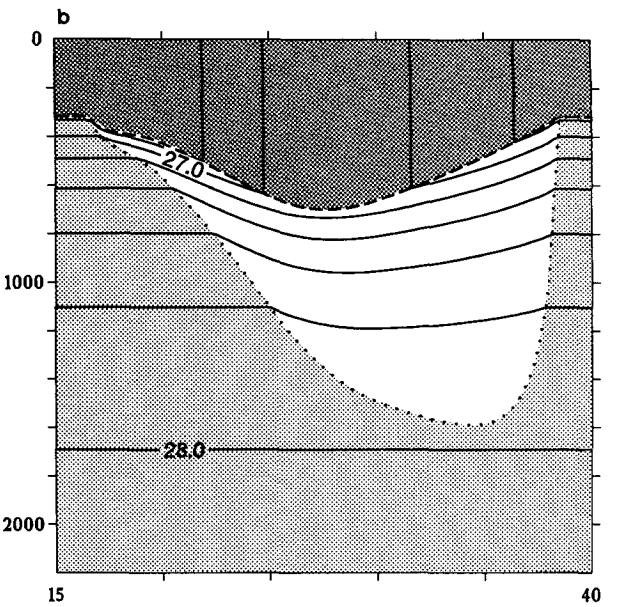

FIG. 9. Results for the "narrow throat" experiment. (a) Contours of surface density ρ_m, in terms of $\sigma = \rho - 1000$. (b) A meridional section at 55°W. (c) The S field in units of meters per year.

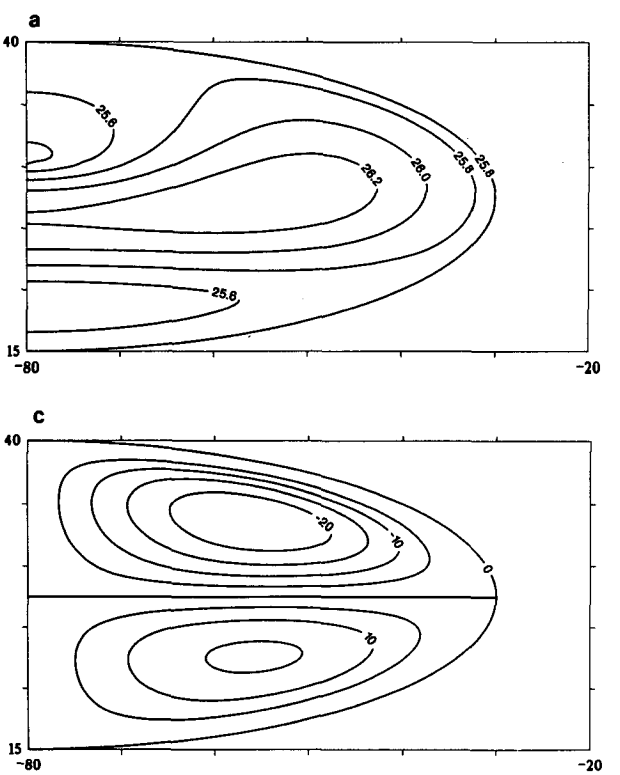

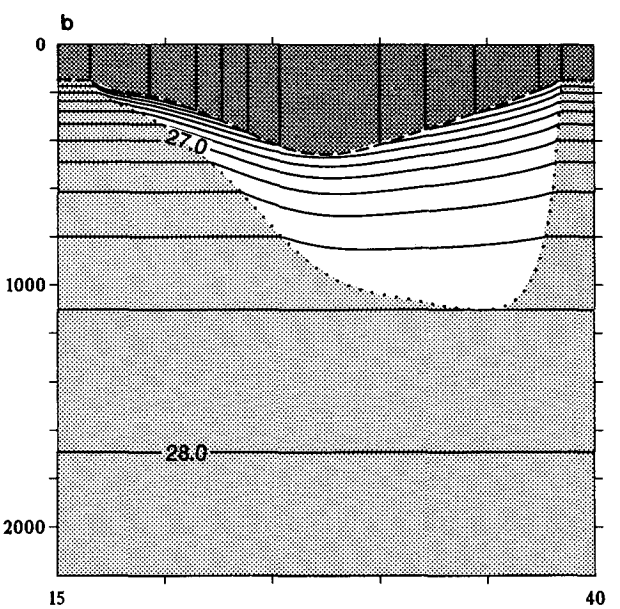

FIG. 10. Results for the "realistic" case. (a) Contours of surface density ρ_m, in terms of $\sigma = \rho - 1000$. (b) A meridional section at 55°W. (c) The S field in units of meters per year.

now thinner, the stratification just below the mixed-layer base is much stronger than in the previous two cases.

To thin the mixed layer, in a manner consistent with the reference stratification (16), we choose a mixed-layer density outside the gyre ρ_{mo} of 1025.8 (this leads to a mixed layer 150-m thick outside the gyre), and the northwestern boundary condition (15) warming toward the south (to prevent the mixed layer in the center of the gyre from becoming too dense).

We choose a surface heating with precisely the same form as in (14), (Fig. 6), but twice as strong; thus, $\mathscr{H}^*_{\text{net}} = 400$ W m^{-2} and $\mathscr{H}_{\text{net}}$ reaches a maximum magnitude of ~ 35 W m^{-2}.

The resulting surface density field (Fig. 10a) again shows the warm water at the southern edge of the inflow, the cold pool in the center of the gyre, and the rewarmed waters to the south. Absolute values of density are, of course, everywhere considerably less—consistent with the much thinner mixed layer (300 m rather than 600 m thick) evident in the meridional 55°W section, Fig. 10b. The thinner mixed layer, together with the reference stratification that steepens toward the surface, implies, as is evident in Fig. 10b, very high values of stratification just below the mixed-layer base—up to 6–9 kg m^{-3}/km. Thus, even though the heat input, twice as strong as in the previous case, colludes with the thinner mixed layer to produce a much greater heat flux convergence and hence $D_b\rho_m/Dt$, subduction rates (Fig. 10c) differ little—compared with Fig. 9c.

We now consider the interesting special case where there is *no* mixed layer and the Ekman layer pumps fluid directly into and out of the thermocline.

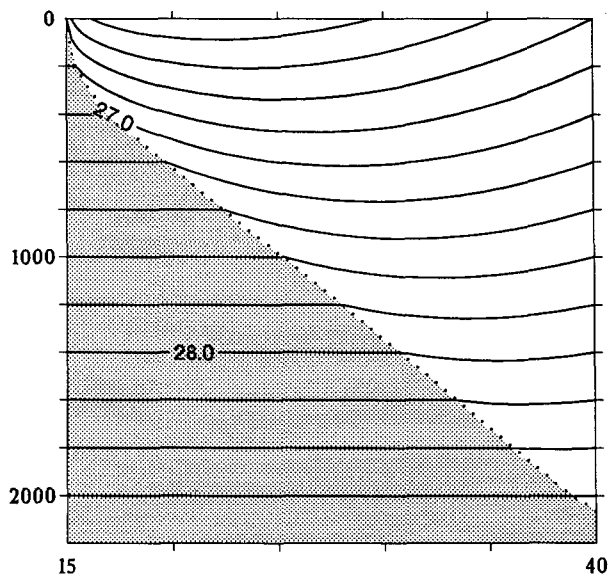

FIG. 11. Meridional section through a homogenized gyre with no mixed layer.

b. A mixed layer of zero thickness

Let us now consider the degenerate case in which the mixed layer vanishes. Figure 11 is a meridional vertical section through such a gyre, where a zero mixed-layer thickness has been *imposed.* Wind forcing and stratification are as in section 3a (1).

From the kinematic definition of S, (1), it is clear that as $h \to 0$, $S \to -w_b \to -w_e$; the subduction rate must tend to the Ekman pumping rate. Substituting $S = -w_e$ into the thermodynamic expression for S, (12), implies that as $h \to 0$, the heat flux *convergence* $\mathscr{H}_{\text{net}}/h$ remains finite; this finite convergence exists over a layer of vanishing thickness, and so the net heat *flux* $\mathscr{H}_{\text{net}}$ disappears.

Rather than passing into a mixed layer, all of the Ekman pumping must be subducted directly into the thermocline, into those layers of density $\sigma < 26.6$ (see Fig. 11). These layers form the ventilated thermocline. This solution is, in fact, Rhines and Young's (1982) homogenized gyre.

4. Concluding remarks

The Ekman layers set up by the prevailing wind patterns pump fluid into and out of the mixed layer, driving a lateral flow that slides almost horizontally to and from the thermocline through the base of the sloping mixed layer. We have precisely defined this subduction flux S, Eq. (1), and made its connection with the diabatic heating, mixed-layer depth and thermocline stratification, explicit and quantitative through Eq. (12).

In particular, we note the following.

1) Our central result $S = \alpha_E f \mathscr{H}_{\text{net}}/hC_w\bar{\rho}Q_b$ permits time dependence.

2) Here, S does not depend explicitly on the Ekman pumping field; indeed S can have the *opposite* sign to w_e.

3) The sign of S depends on $f\mathscr{H}_{\text{net}} = \mathscr{H}_{\text{in}} - (C_w/\alpha_E\bar{\rho}f)\mathbf{k} \times \tau \cdot \nabla\rho_m$, the total heat flux through the sea surface less the advection by the Ekman drift, rather than $\mathscr{H}_{\text{in}}$, the total heat flux through the sea surface. Thus, if $\mathscr{H}_{\text{in}}$ merely supplies sufficient heat to allow the Ekman drift to cross the surface density contours, so that $\mathscr{H}_{\text{net}} = 0$, then $S = 0$. If $\mathscr{H}_{\text{net}} > 0$, $S > 0$; if $\mathscr{H}_{\text{net}} < 0$, $S < 0$.

4) The magnitude of S depends on $\mathscr{H}_{\text{net}}/hQ_b$ and so is dependent on the strength of the thermodynamic forcing but also, and perhaps critically, on the depth and stratification at the base of the mixed layer.

5) The flux of potential vorticity from the mixed layer SQ is proportional to $f\mathscr{H}_{\text{net}}/h$.

The above points have been illustrated by making use of MN's steady thermocline model driven by prescribed patterns of Ekman pumping and diabatic heating. The model vividly demonstrates that S can be very different from w_e, both in magnitude and sense. The

field of Ekman pumping sets up the sense of the depth-integrated flow of the gyre (through the Sverdrup constraint), but the sense of flow between the mixed layer and the thermocline is controlled by the net heating. In the examples modeled here, we have chosen to prescribe the heating as a fixed function of space, but it should be remembered that in nature the heating field is not flow independent, and, furthermore, it changes with the seasons. In particular, the time of year when S reaches a maximum depends on the magnitude of the heating modulated by $1/hQ_b$. Although $\mathscr{H}_{\text{net}}$ has a maximum at the summer solstice when the mixed-layer depth is a minimum, the stratification at its base is likely to be strong, tending to cut off subduction; the exact phase of S relative to the seasonal cycle is as yet unclear.

Finally, Eq. (12) may have some diagnostic value for studying the field of S from observations. Work is proceeding to compute S over the North Atlantic using Isemer and Hasse's (1987) estimate of $\mathscr{H}_{\text{in}}$ and the mixed-layer depths and potential vorticity at the base of the mixed layer deduced from the climatological hydrographic data.

REFERENCES

Cushman-Roisin, B., 1987: Dynamics of the oceanic surface mixed layer. *Hawaii Institute of Geophysics Special Publications,* P. Muller and D. Henderson, Eds.

Federiuk, J. M., and J. F. Price, 1985: Mechanisms of oceanic subduction. Unpublished manuscript.

Isemer, H.-G., and L. Hasse, 1987: *The Bunker Climate Atlas of the North Atlantic Ocean, Vol. 2: Air-Sea interactions.* Springer-Verlag.

Luyten, J. R., J. Pedlosky, and H. Stommel, 1983: The ventilated thermocline. *J. Phys. Oceanogr.,* **13,** 292–309.

Marshall, J. C., and A. J. G. Nurser, 1991: A continuously stratified thermocline model incorporating a mixed layer of variable thickness and density. *J. Phys. Oceanogr.,* **21,** 1780–1792.

Nurser, A. J. G., 1988: On the distortion of a baroclinic Fofonoff gyre by wind-forcing. *J. Phys. Oceanogr.,* **18,** 243–257.

Rhines, P. B., 1986: Lectures on ocean circulation dynamics. *Large-Scale Transport Processes in Oceans and Atmosphere,* J. Willebrand and D. L. T. Anderson, Eds., Reidel, 105–161.

——, and W. R. Young, 1982: A theory of the wind-driven circulation. I: Mid-ocean gyres. *J. Mar. Res.,* **40**(Suppl), 559–596.

Williams, R. G., 1989: The influence of air–sea interaction on the ventilated thermocline. *J. Phys. Oceanogr.,* **19,** 1255–1267.

Woods, J. D., 1985: The physics of thermocline ventilation. *Coupled Atmosphere–Ocean Models,* J. C. J. Nihoul, Ed., Elsevier.

——, and W. Barkmann, 1988: A Lagrangian mixed-layer model of Atlantic 18°C water formation. *Nature,* **319,** 574–576.